Virology 419 (2011) 43–53

Contents lists available at ScienceDirect

Virology

journal homepage: www.elsevier.com/locate/yviro

Molecular characterization of *Drosophila* cells persistently infected with Flock House virus

Juan Jovel *, Anette Schneemann **

Department of Molecular Biology, The Scripps Research Institute, La Jolla, CA 92037, USA

ARTICLE INFO

Article history:
Received 26 April 2011
Returned to author for revision 6 June 2011
Accepted 4 August 2011
Available online 26 August 2011

Keywords:
Flock House virus
Persistent infection
Defective RNA
RNA interference

ABSTRACT

Little is known about the molecular determinants causing and sustaining viral persistent infections at the cellular level. We found that *Drosophila* cells persistently infected (PI) with Flock House virus (FHV) invariably harbor defective viral RNAs, which are replicated by the FHV RNA-dependent RNA polymerase. Some defective RNAs encoded a functional B2 protein, the FHV suppressor of RNA interference, which might contribute to maintenance of virus persistence. Viral small interfering RNAs (vsiRNAs) of both polarities were detected in PI cells and primarily mapped to regions of the viral genome that were preserved in the isolated defective RNAs. This indicated that defective RNAs could represent major sources of vsiRNAs. Immunofluorescence analysis revealed that mitochondria and viral proteins are differentially distributed in PI cells and lytically infected cells, which may partly explain the reduction in infectious viral progeny. Our results provide a basis for further investigations of the molecular mechanisms underlying persistent infections.

Introduction

During evolution, metazoans have acquired a multitude of defense mechanisms that protect them against deleterious effects from pathogenic viruses. In spite of this, a number of viruses infecting diverse organisms are able to resist these defenses and establish persistent infections (Britt, 2008; Dasgupta et al., 1994; Fuse et al., 2008; Kuno, 2001; Oldstone, 2006). The molecular mechanisms underlying establishment of persistent infections remain incompletely understood, but they are likely based on an equilibrium between host defense responses and the counter-responses by the virus.

Insects, including *Drosophila*, rely mainly on the RNA interference (RNAi) pathway to combat viral infections (Aliyari et al., 2008; Blair, 2011; Ding, 2010; Galiana-Arnoux et al., 2006; Huszar and Imler, 2008; Kemp and Imler, 2009; Wang et al., 2006). In general, the RNAi pathway is triggered by double-stranded RNA (dsRNA), which is sensed by the RNase III-like enzyme Dcr-2 (Carthew and Sontheimer, 2009; Ding, 2010; Kim et al., 2006; Lee et al., 2004) and subsequently cleaved into 21-nt-long small interfering RNAs (siRNAs). Dcr-2 and R2D2, an RNA binding protein (Liu et al., 2003), constitute a loading complex that incorporates siRNAs into a multiprotein RNA-induced silencing complex, RISC (Marques et al., 2010; Okamura et al., 2011). RISC is responsible for degradation of single-stranded RNA molecules bearing sequence complementarity to the guide strand of the siRNA (Ding, 2010; Kim et al., 2007; Rand et al., 2005). The effector molecule in the RISC complex is AGO2, an RNase H-like enzyme (Hammond et al., 2001; Rand et al., 2005; van Rij et al., 2006). HEN1, a methyltransferase that modifies siRNAs at their 3′-end, has also been shown to be essential for RISC activation in some endogenous small RNA pathways (Ding, 2010; Ding and Voinnet, 2007; Horwich et al., 2007).

Flock House virus (FHV) is a positive-sense, single-stranded RNA virus [(+)ssRNA] that has a bipartite genome composed of RNA1 (3107 nt) and RNA2 (1400 nt). RNA2 encodes the capsid protein whereas RNA1 encodes the viral RNA-dependent RNA polymerase (RdRp). RNA1 also gives rise to subgenomic RNA3 during replication (Guarino et al., 1984). RNA3 serves as the mRNA for synthesis of protein B2, a potent viral suppressor of RNAi (VSR). Structural and biochemical analyses of B2 have shown that it is a dsRNA binding protein. It interferes with RNAi by protecting long dsRNAs from cleavage by Dcr-2 and inhibiting incorporation of viral siRNAs into RISC (Aliyari et al., 2008; Chao et al., 2005; Korber et al., 2009).

FHV infects and kills adult *Drosophila* flies (Galiana-Arnoux et al., 2006; Wang et al., 2006) and can be propagated in cultured *Drosophila* line 1 (DL-1) and line 2 (S2) cells. Extensive lysis is observed for infected DL-1 cells and to a lesser extent for S2 cells. Both types of cell produce exceptionally large amounts of progeny virions that form paracrystalline arrays in the cytoplasm late in infection (Lanman et al., 2008). For S2 cells, the burst size has been estimated to be on the order of 250,000 progeny particles per cell (Scotti et al., 1983).

Despite its potent suppression of the cellular RNAi response and its generally lytic properties, FHV readily establishes persistent infections in cultured *Drosophila* cells. It was initially reported that 1% of FHV-

* Correspondence to: J. Jovel, Dept. Plant Pathology, University of California Riverside, 3401 Watkins Dr., Riverside, CA 92521, USA.
** Correspondence to: A. Schneemann, Dept. of Mol. Biology, The Scripps Research Institute, 10550 N. Torrey Pines Rd, La Jolla, CA 92037, USA. Fax: +1 858 784 7979.
E-mail addresses: jjovel@catie.ac.cr (J. Jovel), aschneem@scripps.edu (A. Schneemann).

0042-6822/$ – see front matter © 2011 Elsevier Inc. All rights reserved.
doi:10.1016/j.virol.2011.08.002

infected *Drosophila* cells survive an infection and emerge in a persistently infected state (Dasgupta et al., 1994). These cells produce small amounts of infectious FHV particles and are resistant to superinfection with FHV and the closely related nodaviruses Black Beetle virus and Boolaravirus. In contrast, they are not resistant to superinfection with genetically unrelated viruses such as Cricket paralysis virus (CrPV), a dicistrovirus, and *Drosophila* X virus, a birnavirus (Selling, 1986). This observation indicates that the RNAi machinery may play a role in the maintenance of the persistently infected phenotype.

In this study, we have extensively characterized four independently established *Drosophila* DL-1 cell lines persistently infected with FHV. Our results strongly suggest that the cells use RNAi to control viral replication and that defective RNAs are likely major contributors to formation of viral small interfering RNAs (vsiRNAs). Finally, we demonstrate that the cellular distribution of FHV proteins in persistently infected cells differs markedly from that observed in lytically infected cells. Our results provide a foundation for future studies to determine the molecular mechanism that permits establishment of nodavirus persistence in *Drosophila* cells.

Results

Generation and biochemical characterization of Drosophila cells persistently infected with FHV

We generated several independent polyclonal *Drosophila* cell lines that were persistently infected with FHV. To this end, Schneider's *Drosophila* line 1 cells (DL1) were inoculated with gradient-purified FHV at various multiplicities of infection (MOI), namely 0.01, 1, 10 and 100. As previously reported (Dasgupta et al., 1994), most of the cells were killed by the virus but a small percentage survived the infection. The appearance of the surviving cells and their growth rate were indistinguishable from that of uninfected DL-1 cells and they were continually passaged from that point on. We refer to these lines as $PI_{0.01}$, PI_1, PI_{10} and PI_{100}.

To confirm that the PI lines were persistently infected with FHV, cell lysates were prepared and analyzed by SDS-PAGE and immunoblot. In contrast to lytically infected cells, viral proteins were undetectable on stained gels in all PI lines except $PI_{0.01}$, where bands representing the coat protein and the VSR B2 were visible (Fig. 1A, upper panel). More sensitive immunoblot analysis, however, established that all PI lines contained these two proteins indicating that they were infected with FHV (Fig. 1A, lower panel). The reduced viral protein content relative to lytically infected *Drosophila* cells is a characteristic of FHV persistent infection. We furthermore confirmed that PI cell lines produced infectious FHV particles, albeit in much smaller amounts than those detected during lytic infection. Specifically, virus isolated from PI cells gave rise to 10^3 to 10^4 fewer plaques than virus isolated from the same number of lytically infected cells (data not shown).

The level of viral RNA, both positive and negative strands, was established by Northern blot analysis conducted on total RNA samples extracted from PI cells. Total RNA from lytically infected (LI) and

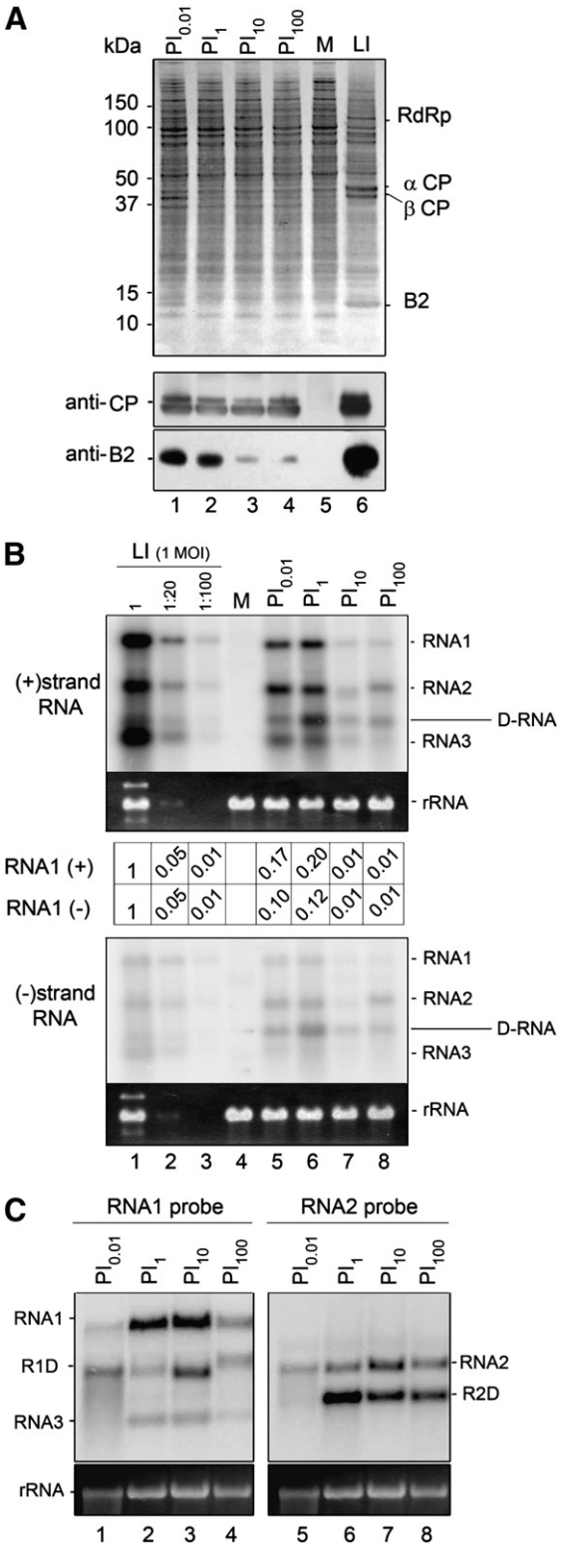

Fig. 1. Detection of FHV proteins and RNA in persistently infected DL1 cells. (A) Detection of FHV proteins. Upper panel: total cellular protein (5 μg) from persistently infected DL1 cells (lanes 1–4), non-infected cells (lane 5) or cells lytically infected at an MOI of 10 (lane 6) were separated by SDS-PAGE and stained with SimplyBlue SafeStain (Invitrogen). Position of viral RdRp, coat protein (CP) and B2 is indicated to the right. Note that CP undergoes a maturation cleavage after assembly and is detected in its precursor form α as well as in the mature form β. Lower panel: immunoblot analysis of identical cell lysates with antibodies against coat protein and B2. (B) Detection of FHV genomic and defective RNAs by Northern blot analysis. Total RNA (5 μg) extracted from lytically infected DL1 cells (lanes 1–3), mock-infected DL1 cells (lane 4) and persistently infected DL1 cells (lanes 5–8) was electrophoresed through a denaturing 1.2% agarose gel, blotted onto nylon membrane and crosslinked. Strand-specific, radioactive probes for hybridization were generated by *in vitro* transcription and spanned ~800 to 900-nt-long stretches in RNA1 (nts 20–834), RNA3 (nts 2251–3107) and RNA2 (nts 25–965). Ethidium bromide (EtBr) staining of the gel prior to transfer reveals the presence of rRNA and is shown as a loading control; note that viral RNA1 and RNA2 are so abundant in lytically infected cells that they are easily detectable above and below rRNA, respectively, in lane 1. Lanes 2 and 3 contain 20-fold and 100-fold less LI RNA, respectively, than what is shown in lane 1. Numbers between the two panels represent relative levels of positive and negative strand RNA1 in LI and PI cells. Quantification was done by phosphorimaging and using the software ImageQuant. D-RNA is defective RNA. (C) Detection of positive strands of FHV RNAs using RNA1-specific (lanes 1–4) or RNA2-specific (lanes 5–8) probes described above. The membrane was probed for the presence of RNA1, stripped, and then probed for the presence of RNA2. R1D is defective RNA derived from RNA1; R2D is defective RNA derived from RNA2.

mock-infected cells served as controls. Similar to viral protein, RNA levels were significantly reduced in PI cells (Fig. 1B, lanes 5–8) compared to LI cells (lanes 1–3). Noticeably, a RNA that migrated faster than RNA2, was also detected in PI cells and appeared to represent a defective RNA. Hybridization analysis using probes specific for detection of RNA1 and RNA2 revealed that putative defective RNAs derived from both genomic segments were present in PI cells (Fig. 1C). Such defective RNAs were not unique to DL1 cells persistently infected with FHV. Using Schneider's *Drosophila* line 2 (S2) cells to generate persistently infected PI cell lines, we observed similarly reduced levels of viral RNAs relative to lytically infected S2 cells as well as the presence of defective RNAs that migrated to a position analogous to that observed for defective RNA in PI cells derived from DL-1 (data not shown).

Differential distribution of FHV proteins in lytically and persistently infected cells

A comparison of lytically and persistently infected DL-1 cells by confocal immunofluorescence microscopy provided further evidence that the levels of coat protein and B2 were considerably reduced in PI cells (Fig. 2A). Interestingly, coat protein, which is known to colocalize with the ER in LI cells (Venter et al., 2009), had a predominantly punctate distribution in PI cells and there was little similarity with the reticular pattern normally detected (Fig. 2A, bottom panel). In many cells, the punctae were enriched in the perinuclear region. These differences prompted more detailed comparisons of the cellular distribution of the three FHV proteins, RdRp, coat protein and B2 in LI and PI cells. In addition, we investigated the distribution of mitochondria, a key organelle involved in the viral replication cycle.

A typical example of the distribution of RdRp, coat protein and mitochondria in LI cells is shown in Fig. 2B (top panel). Coat protein closely followed the ER, whereas mitochondria and RdRp were clustered in the perinuclear area. RdRp is known to be located on the outer membrane of mitochondria (Miller and Ahlquist, 2002; Miller et al., 2001), explaining the overlap of the two signals. The clustering of mitochondria is a hallmark of FHV infection and is thought to be required for efficient assembly of progeny virions near the site of viral RNA synthesis (Venter et al., 2009). In stark contrast, mitochondria and RdRp were evenly distributed in PI cells (Fig. 2B, bottom panel) indicating that the mechanisms normally leading to accumulation of these organelles near the nucleus were not operational. Similar to coat protein and B2 protein, the level of RdRp was significantly lower in PI cells than LI cells.

The cellular distribution of B2 had not been investigated previously. We observed that in LI cells, B2 was primarily localized in the perinuclear area, i.e. the site of viral RNA synthesis. Closer inspection of the images indicated that, in contrast to RdRp, B2 was located adjacent to mitochondria and formed ribbon-like structures that were interspersed between the organelles (Fig. 2C, upper two panels). A lesser, yet significant portion of B2 was located in the cell periphery where it assumed a reticular distribution similar to that of coat protein (Fig. 2C, top panel). The location of B2 in PI cells mirrored the loss of mitochondrial clustering (Fig. 2C, bottom panel). Much of B2 assumed a punctate distribution dispersed throughout the cell, in close vicinity of mitochondria, whereas a smaller portion retained the reticular pattern observed in LI cells.

PI cells contain FHV-derived small interfering RNAs

In persistently infected cells an equilibrium exists between cellular defenses used to control a foreign pathogen and the ability of the pathogen to overcome these defenses. In *Drosophila*, the RNAi pathway is the major response mounted against viral infection but many *Drosophila*-infecting viruses, including FHV, encode proteins that potently suppress RNAi. We therefore investigated whether FHV RNAs were subject to RNA silencing in PI cells. To this end, the presence of viral small RNAs (vsRNAs) was evaluated by Northern blot analysis (Fig. 3A). Large amounts (40 μg) of total cellular RNA had to be employed in order to visualize the vsRNAs, indicating that they were present at low abundance. vsRNAs derived from the genomic as well as antigenomic strand were detectable (Fig. 3A, lanes 1–4, 8–11). These results were consistent with other recent studies (Czech et al., 2008; Flynt et al., 2009) reporting the presence of vsRNAs of both polarities in S2 cells persistently infected with FHV.

To determine whether the presence of vsRNAs indicated ongoing RNAi activity in PI cells, i.e. whether the vsRNAs functioned as viral small interfering RNAs (vsiRNAs), we transfected PI cells with a reporter construct expressing GFP from a derivative of FHV RNA2, called DIeGFP. In contrast to naïve cells, which expressed abundant amounts of GFP when co-transfected with DIeGFP RNA and FHV RNA1, there was little to no GFP detected in PI cells (Fig. 3B). Furthermore, there was little to no evidence of replication of the DIeGFP RNA (Fig. 3C), whereas this RNA was abundant in naïve cells. These results strongly suggested that the reporter construct was inactivated in PI cells by pre-existing components of the RNAi machinery specific for FHV sequences. The notion that the RNAi response in PI cells was active was also supported by the observation that the cells were resistant to superinfection with FHV, whereas challenge with the genetically unrelated Cricket paralysis virus (CrPV) led to full blown infection and cell lysis (data not shown).

Inability of FHV to kill cells in a persistently infected culture could be the result of mutations in the viral RNAi suppressor protein B2, which diminish its capacity to render vsiRNAs inactive. To test this possibility, cDNA of RNA3, the message of protein B2, was prepared from PI cells and 25 independent clones were sequenced. However, no mutations in the B2 open reading frame were detected. These results were in agreement with a recent study using S2 cells persistently infected with FHV (Flynt et al., 2009) and suggest that the PI phenotype is not due to selection of mutant viruses whose RNAi suppressor protein has a reduced ability to sequester vsiRNAs and/or to protect long viral dsRNA from Dicer-2 activity.

Modular distribution of vsiRNAs along the FHV genome is a characteristic property of PI cells

Deep-sequencing of small RNAs from S2 cells persistently infected with FHV recently provided detailed information on the identity and relative abundance of FHV-derived siRNAs in this particular cell line (Czech et al., 2008, 2009; Flynt et al., 2009). Two findings were of special interest. First, roughly equal numbers of plus and minus strand vsiRNAs were detected. Second, vsiRNAs were not evenly distributed along the FHV genome but fell into distinct regions. We sought to investigate whether this distribution pattern is a common feature of *Drosophila* cells persistently infected with FHV or whether it is unique to the S2 line employed in the previous study. To facilitate comparative analyses, a density plot of vsiRNAs from the S2 cell line (Czech et al., 2009) was generated (Fig. 4A). It shows that the majority of vsiRNAs mapped to the 5′ and 3′ terminal regions on FHV RNAs1 and 2 as well as a central region on RNA2.

To map the distribution of vsiRNAs along the FHV genome in our PI cell lines, we used PCR to generate contiguous ~250-nt-long fragments that covered the entire RNA1 and RNA2 (Fig. 4B). These fragments were transferred to a nylon membrane under denaturing conditions. As a negative control, a 250-nt-long fragment of Nodamura virus (NoV), another nodavirus, was also included (fragment 19 in Fig. 4C). Small RNAs, 18–24 nts in length, were then isolated from lines $PI_{0.01}$, PI_1, PI_{10} and PI_{100} as well as from LI cells at 12, 24 and 36 h post infection (hpi). The RNAs were dephosphorylated, radioactively end-labeled and used as probes for hybridization to the PCR fragments.

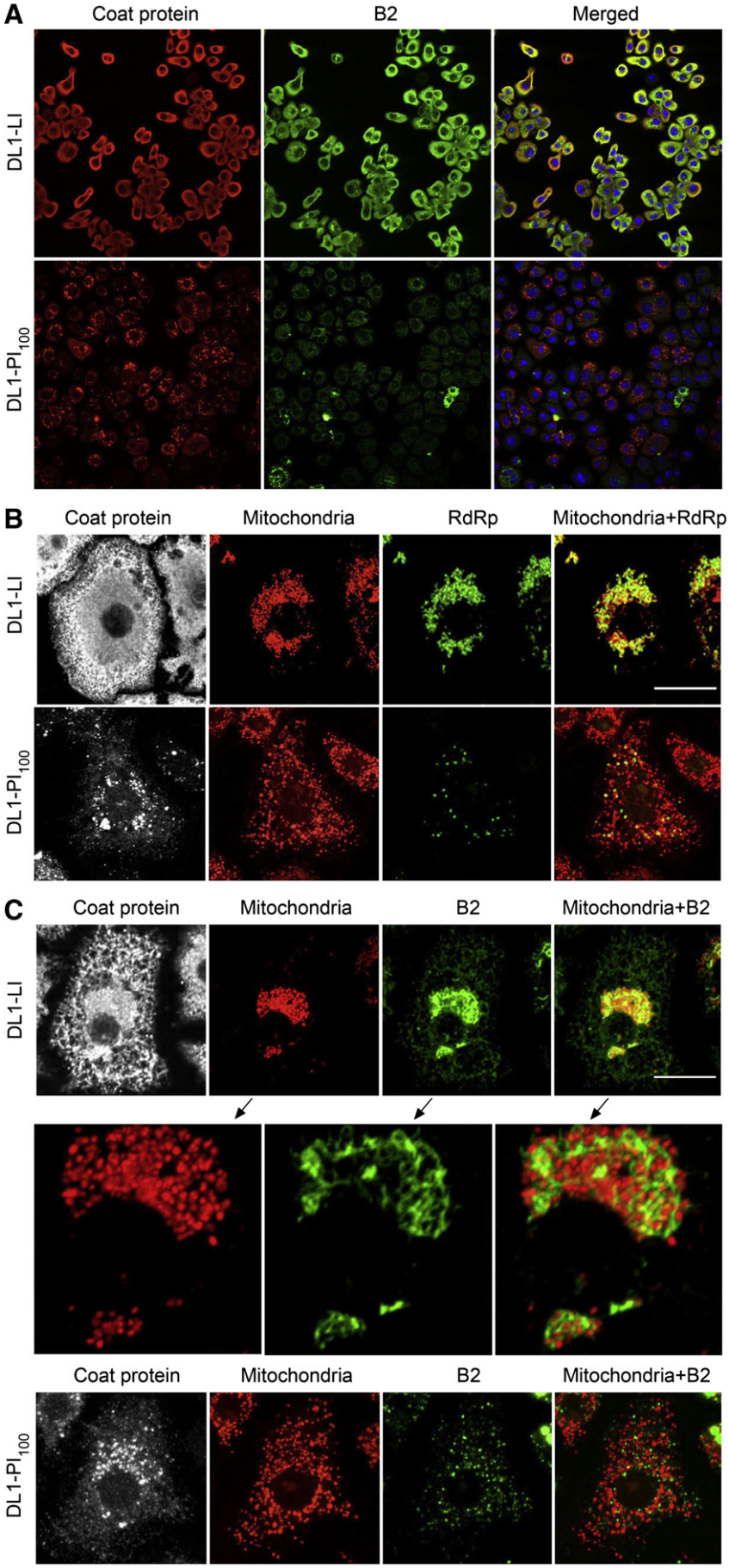
A
Coat protein
B2
Merged
DL1-LI
DL1-PI100
B
Coat protein
Mitochondria
RdRp
Mitochondria+RdRp
DL1-LI
DL1-PI100
C
Coat protein
Mitochondria
B2
Mitochondria+B2
DL1-LI
Coat protein
Mitochondria
B2
Mitochondria+B2
DL1-PI100

In the case of LI cells, the distribution of vsiRNAs that mapped to RNA1 was relatively uniform at 12 hpi, although vsiRNAs mapping to fragments 4, 5 (nts 750–1250) and 12 (nts 2751–3107) were somewhat more abundant given the stronger hybridization signals (Fig. 4C). By 24 hpi, the relative levels of vsiRNAs hybridizing to these fragments as well as fragments 9–11 (nts 2001–3107) had clearly increased and by 36 hpi the majority of vsiRNAs mapped to a 5′ terminal region (fragment 1, nts 1–250), a central region (fragments 4–6, nts 750–1500) and a 3′ terminal region (fragments 8–12, nts 1750–3107). In contrast, hybridization of vsiRNAs to fragments representing RNA2 remained uniform with no particular pattern discernible during the course of infection.

The situation was clearly different in PI cells. When small RNAs from the four PI lines were analyzed in the same way a very different, albeit consistent, pattern was detected. Specifically, vsiRNAs mapping to RNA1 formed three clusters represented primarily by fragment 1 (nts 1–250), fragments 4–5 (nts 751–1250) and fragments 11–12 (nts 2501–3107) (Fig. 4C). Except for the central region containing nts 751–1250, this pattern matched that observed for vsiRNAs in the persistently infected S2 cell line. Similarly, vsiRNAs mapping to RNA2 formed three clusters represented primarily by fragment 13 (nts 1–250), fragment 15 (nts 501–750) and fragment 18 (1251–1400). Once again, this distribution closely matched that reported for persistently infected S2 cells (Czech et al., 2008; Flynt et al., 2009). The modular and reproducible distribution pattern of vsiRNAs along the viral genome is thus a characteristic of *Drosophila* cells persistently infected with FHV.

Characterization of defective RNAs isolated from PI cell lines

FHV defective RNAs and defective-interfering RNAs are spontaneous deletion mutants of the full-length genomic RNA segments. In general, they do not encode functional proteins but can replicate in the presence of FHV RdRp. Analysis of their primary structure has revealed that the 5′ and 3′ ends of RNA1 and RNA2 are always retained in defective RNAs. In addition, defective RNAs derived from RNA2 contain a central region, approximately representing nts 520–730, of the parental segment (Ball and Li, 1993; Li and Ball, 1993; Zhong et al., 1992). We noticed that vsiRNAs in PI cells mapped predominantly to regions conserved in defective RNAs and wondered whether defective RNAs played a role in maintaining the state of viral persistence, for example by representing a source for the generation of vsiRNAs as well as a target for RISC. To investigate this further, we isolated and characterized defective RNAs associated with our PI cell lines.

Specifically, total RNA from the four PI lines was pooled and subjected to RT-PCR using primers that either mapped to the 5′ and 3′ ends of RNA1 or RNA2. Amplification products whose size was smaller than those resulting from full-length viral RNAs 1 and 2 were isolated, cloned and sequenced. Out of 20 independent clones analyzed, three were derived from RNA1 and 12 were derived from RNA2. The remaining 5 clones lacked motifs known to be essential for FHV replication (Ball and Li, 1993; Li and Ball, 1993; Zhong et al., 1992) and were not included in subsequent investigations.

The three clones containing sequences derived from RNA1 were identical and their structure is shown in Fig. 5. We refer to this clone as $R1D_{1626}$ based on the number of RNA1-derived nucleotides contained in this isolate. $R1D_{1626}$ was composed of five fragments encompassing nucleotides 1–311, 1096–1143, 1190–1305, 1951–2569 and 2576–3107 of full-length genomic RNA1 (Fig. 5).

The 12 clones representing RNA2 fell into three classes: $R2D_{660}$ (8/12), $R2D_{675}$ (3/12) and $R2D_{567}$ (1/12) (Fig. 5). All three classes of R2Ds retained at a minimum the following nucleotides of full-length genomic RNA2: 1–59, 63–94, 224–240, 525–728, 1220–1352 and 1378–1400. The 3′ terminal fragment invariably contained a small insertion after nt 1352, 1357 or 1358 that represented a region normally located near the 5′ end (Fig. 5).

Interestingly, when the vsiRNAs profiled in Fig. 4A were mapped to the sequence of the defective RNA molecules, a relatively uniform distribution was observed for defective RNAs derived from RNA2 (Fig. 6). This was in contrast to the three clusters found along the sequence of full-length RNA2. On $R1D_{1626}$ the vsiRNAs also mapped more uniformly although relatively few corresponded to the central region.

Defective RNAs isolated from PI cells are replicated by FHV RdRp

We confirmed that the FHV RNA deletion mutants identified in the PI cell lines represented *bonafide* defective RNAs by showing that they served as a template for replication in the presence of FHV RdRp. To this end, *in vitro* transcripts of all defective RNAs were generated and transfected into naïve DL1 cells together with wild type RNA1 (R1wt). Northern blot analysis revealed abundant positive and negative strands of defective RNAs as well as positive and negative strands of R1wt and its subgenomic RNA3 (Fig. 7A, lanes 3–7 and 11–15).

In the absence of R1wt, none of the defective RNAs replicated. This was expected for the defective RNAs derived from RNA2 as this segment does not encode any replication functions. The fact that $R1D_{1626}$ was also unable to replicate in the absence of R1wt (Fig. 7A, lanes 2 and 10) indicated that the open reading frames on $R1D_{1626}$ no longer encoded a functional polymerase protein. Surprisingly, $R1D_{1626}$ accumulated to high levels when it was co-transfected with transcripts of R1ΔB2, a mutant form of RNA1 that encodes a functional polymerase but does not express the RNAi suppressor protein B2 (Fig. 7A, lanes 4 and 12). R1ΔB2 transcripts by themselves are unable to sustain replication in DL1 cells (Fig. 7A, lanes 1 and 9) because they are cleared by the cellular RNAi response. In the presence of $R1D_{1626}$, however, replication products of R1ΔB2 were clearly detectable. Inspection of the $R1D_{1626}$ sequence revealed that the region representing the subgenomic RNA3 was retained (Fig. 7B) implying that $R1D_{1626}$, in principle, could give rise to protein B2. Indeed, Western blot analysis confirmed that cells co-transfected with R1ΔB2 and $R1D_{1626}$ contained appreciable amounts of B2 (Fig. 7B, lane 4) and suggested that $R1D_{1626}$ and R1ΔB2 were mutually dependent on each other for accumulation in DL1 cells. The reason for the much higher replication efficiency of $R1D_{1626}$ relative to R1ΔB2 is not known.

The B2 open reading frame on $R1D_{1626}$ was not necessary for replication of this defective RNA. When this reading frame was closed by mutagenesis, replication of $R1D_{1626}$ was still detectable in the presence of R1ΔB2 in DL1 cells, albeit only when these cells were also treated with dsRNA against AGO2 mRNA to inhibit RNA silencing (Fig. 7C).

Expression of protein B2 in trans does not increase viral replication in PI cells

We next sought to investigate whether defective RNAs are responsible for maintenance of FHV persistence in *Drosophila* cells.

Fig. 2. Subcellular distribution of FHV proteins in lytically and persistently infected DL-1 cells. (A) Comparison of the distribution pattern of FHV coat protein (red) and B2 protein (green) in LI cells (top panel) and PI_{100} cells (bottom panel). Results for $PI_{0.1}$ and PI_{10} were identical to those of PI_{100} (not shown). (B) Close-up view revealing differences in subcellular distribution of coat protein (grayscale), mitochondria (red) and RdRp (green) in LI cells and PI_{100} cells. (C) Top panel: close-up view revealing subcellular distribution of coat protein (grayscale), mitochondria (red) and B2 protein (green) in LI cells. B2 largely co-localizes with mitochondrial signal but a smaller fraction is detected elsewhere in the cytoplasm. Middle panel: zoom-in view of mitochondria shown in top panel. Note that signals for mitochondria and B2 do not overlap. Instead, B2 appears to be interspersed between mitochondria. Bottom panel: subcellular distribution of coat protein (grayscale), mitochondria (red) and B2 (green) in PI_{100} cells. Viral proteins were labeled with specific polyclonal or monoclonal primary antibodies and AlexaFluor conjugated secondary antibodies as described in Experimental procedures. Mitochondria were stained with MitoTracker Red and nuclei with DAPI. All images represent maximal intensity Z-series projections of optical sections. Scale bar is 10 μm.

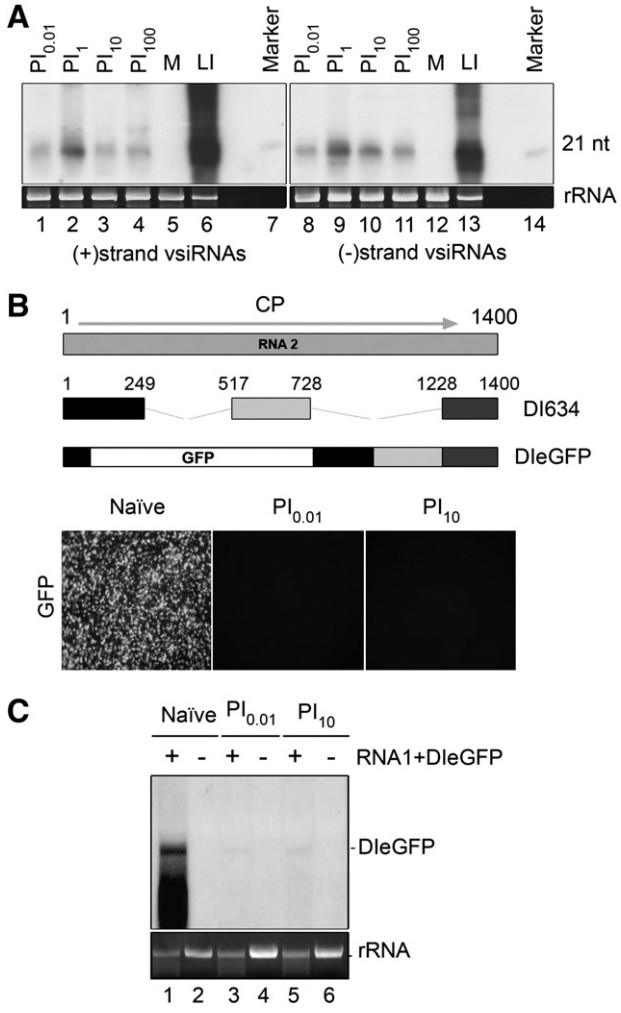

Fig. 3. Persistently infected cells harbor virus-derived small RNAs that inhibit accumulation of a FHV-derived sensor construct. (A) Detection of FHV viral small interfering RNAs (vsiRNAs). Total RNA (40 μg) was separated by PAGE, electroblotted onto positively charged nylon membrane and crosslinked (lanes 1–14). Probes for hybridization were as described in the legend to Fig. 1. RNA from cells lytically infected with FHV at an moi of 20 (lanes 6 and 13) and from mock-inoculated cells (lanes 5 and 12) was used as a positive and negative control, respectively. A 21-mer ribo-oligonucleotide end-labeled with [γ-^{32}P]ATP was used as size marker (lanes 7 and 14). rRNA stained with EtBr is shown as a loading control. (B) Schematic diagram illustrating the structure of sensor construct DIeGFP, a derivative of DI634, used to probe the proficiency of PI cells to silence transcripts containing FHV sequences. Naïve DL-1 cells or PI cells from lines $PI_{0.01}$ and PI_{10} were co-transfected with equal amounts (1 μg) of *in vitro* transcripts of DIeGFP and FHV RNA1 and expression of GFP was evaluated by fluorescence microscopy 48 h later. (C) Northern blot analysis of total RNA extracted from naïve DL-1 cells or PI cells from lines $PI_{0.01}$ and PI_{10} transfected with DIeGFP RNA and FHV RNA1 (lanes 1–6). A radiolabeled DNA fragment corresponding to the full-length eGFP gene was used as a probe. Ribosomal RNA is shown as a loading control.

Specifically, we attempted to eliminate defective RNAs from PI cells by transfecting the cells with siRNAs that specifically targeted the defective RNAs for degradation but not full-length genomic RNAs or the subgenomic RNA3. To this end, we took advantage of unique sequences in defective RNAs located at the junctions where sections of RNA1 or RNA2 are joined and that are non-contiguous in the parental molecules. However, we were unable to detect any appreciable downregulation of defective RNAs using these siRNAs and therefore were not able to address this possibility (data not shown).

In an alternative approach, we investigated whether persistent infection could be turned into lytic infection by artificially increasing the amount of the viral RNAi suppressor protein B2. To test this, we expressed a His-tagged version of B2 *in trans* from an expression plasmid. The His-tag allowed distinction between the exogenous B2 and that expressed from endogenous viral RNA. Not surprisingly, expression of FHV B2-His from an expression plasmid in PI cells failed, presumably because these cells contained RISC complexes specific for the B2 message (Fig. 8A).

To circumvent this problem, we chose to express the B2 protein of NoV that is genetically sufficiently distinct from FHV so that its sequences are not expected to be targeted by FHV-derived siRNAs. The high resolution structure of the FHV and NoV B2 proteins is analogous (Chao et al., 2005; Korber et al., 2009) and their mechanism of siRNA inactivation can be presumed to be identical. Expression of FHV B2-His and NoV B2-His in uninfected DL-1 cells gave rise to easily detectable protein at similar levels (Fig. 8A). In contrast to FHV B2-His, however, the NoV B2-His was also easily expressed in PI cells and observed at similar levels to those in uninfected cells.

Supplementing endogenous levels of FHV B2 in PI cells with NoV B2-His, however, had no effect on FHV accumulation as neither viral RNA (Fig. 8B) nor coat protein (Fig. 8A) showed any appreciable increase. Moreover, PI cells expressing NoV B2-His protein showed no obvious cytopathic effects resembling lytic infection such as cell fragmentation and lysis.

Discussion

In the mid 1980s it was reported that *Drosophila* cells persistently infected with the nodavirus black beetle virus were resistant to superinfection with genetically related viruses such as FHV, but remained fully susceptible to genetically unrelated viruses (Selling, 1986). It remained unclear at that time what the mechanistic foundation for these observations was. In light of the recent discovery of RNA interference and the finding that nodaviral protein B2 functions as a suppressor of RNAi, we hypothesized that nodaviral persistence in cultured cells may be the result of an equilibrium established between the RNAi response by the host and its suppression by the virus.

To investigate this possibility in a systematic fashion, we generated several independent DL-1 cell lines persistently infected with FHV. As predicted, these PI cells produced low amounts of the viral proteins and gave rise to low yields of infectious progeny virus particles. Similarly, PI cells harbored reduced levels of the genomic viral RNAs, but contained significant amounts of defective RNAs, which are not typically observed during lytic infection. Our subsequent investigations led us to propose that defective RNAs may play an important role in maintenance of the persistently infected phenotype through their capacity to serve as a source of viral siRNAs.

We found vsiRNAs of both polarities in our PI cell lines, similar to what has been reported for S2 cells following infection with the VSR-deficient FHVΔB2 virus, a viral mutant that does not encode B2 protein (Aliyari et al., 2008), and several laboratory S2 lines found to be persistently infected with FHV (Flynt et al., 2009). The vsiRNAs in our lines were not evenly distributed along the viral genome but mapped more densely to regions that constitute the defective RNAs isolated and characterized in this study. This suggests that the defective RNAs might be major substrates of the Dcr-2 protein, which is the canonical *Drosophila* enzyme implicated in processing long double-stranded RNA into siRNAs (Carthew and Sontheimer, 2009; Ding, 2010). Defective RNAs may thus serve as attenuators of virus accumulation by providing abundant vsiRNAs, which in turn have the potential to target genomic viral RNAs for degradation. Interestingly, the vsiRNA profile in our cell lines appears to be a conserved feature of *Drosophila* cells persistently infected with FHV, since deep-sequencing of small RNAs from independent libraries and several other PI cell lines yielded the same vsiRNA pattern (Flynt et al., 2009; van Rij and Berezikov, 2009; Wu et al., 2010).

That the RNAi pathway in DL-1 cells persistently infected with FHV is active was also evident by the fact that the DIeGFP construct failed to replicate and express GFP protein. Similarly, a construct intended to transiently express FHV B2 protein in PI cells was inactive in that regard.

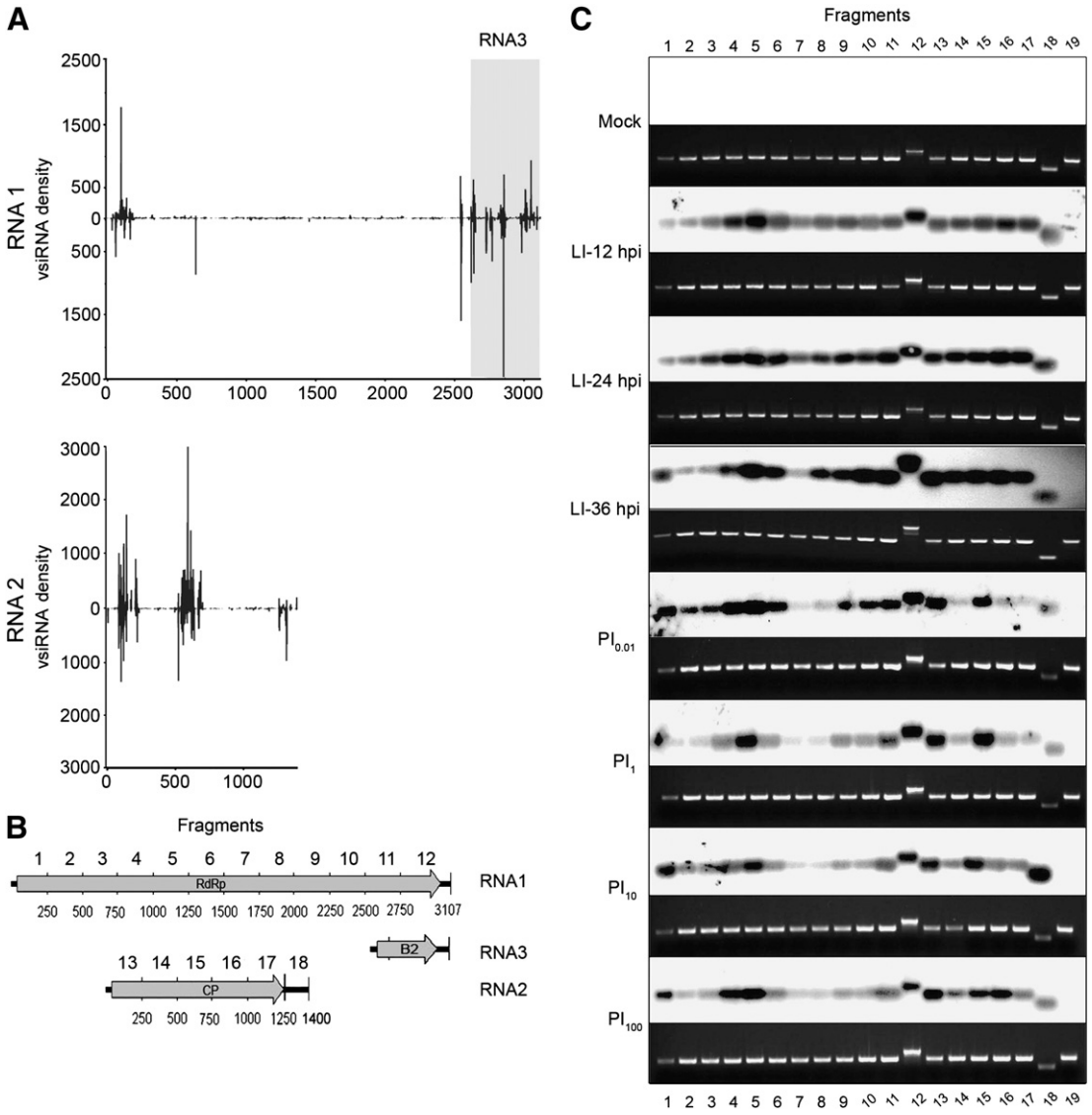

Fig. 4. Profile of vsiRNAs in lytically and persistently infected DL-1 cells. (A) Density plot of FHV vsiRNAs from persistently infected S2 cells described in a previous study (Czech et al., 2009). The region of RNA1 giving rise to the subgenomic RNA3 is shaded in gray. (B) Schematic diagram of PCR fragments used for mapping of vsiRNAs in the current study. (C) Mapping of vsiRNAs along the FHV genome. Lane numbers correspond to PCR fragments shown in panel B. vsiRNAs were extracted at 12 hpi (LI-12 hpi), 24 hpi (LI-24 hpi) or 36 hpi (LI-36 hpi) from DL-1 cells lytically infected with FHV at an moi of 1. Additionally, vsiRNAs were isolated from four different DL1 cell lines persistently infected with FHV. vsiRNAs were radioactively labeled and hybridized to DNA fragments representing defined portions of FHV RNA1 and RNA2. For each blot, the corresponding EtBr-stained gel is presented as a loading control. A 250-nt-long NoV fragment was loaded in the rightmost lane as a negative control.

In contrast, a plasmid for expression of NoV B2 ORF produced abundant B2 protein in both naïve and PI cells. Presumably PI cells contained FHV vsiRNAs integrated into RISC complexes that readily inactivated homologous transcripts, but were ineffective against the heterologous NoV sequence. These observations would explain why PI cells are resistant to superinfection with the same or genetically related viruses but susceptible to heterologous viruses. For example, we found that PI cells could not be superinfected with FHV but remained fully susceptible to infection with the dicistrovirus CrPV.

The ability of vsiRNA-containing RISC complexes to efficiently target RNAs containing FHV sequences, however, was inconsistent. For example, sensor constructs incorporating various 200 nt fragments of RNA1 or RNA2 in their 3′UTR were only marginally silenced in PI cells, regardless of whether the cells contained a high or low level of vsiRNAs mapping to the fragment in question (data not shown). This result, although baffling and in need of further investigation, was reminiscent of data reported by Flynt et al. who suggested that reduced levels of methylation of vsiRNAs may account for the low potency they exhibited to silence homologous sequences in the context of sensor transcripts (Flynt et al., 2009).

We isolated a series of defective RNAs from PI cells, all of which were able to replicate provided that FHV RdRp was supplied *in trans*. Interestingly, $R1D_{1626}$ retained the ability to express functional B2 protein via the subgenomic RNA3. Its sequence also contained two open reading frames encompassing the portion of RdRp that is embedded in the outer mitochondrial membrane as well as the entire polymerase domain (Miller and Ahlquist, 2002). If these fragments are expressed, they might disturb the function of wild type viral proteins and further reduce viral replication efficiency and/or encapsidation. For flaviviruses, it has been proposed that truncated versions of viral proteins are the cause of persistent infections (Catteau et al., 2003; Prikhod'ko et al., 2001). Indeed, even point mutations are able to induce and sustain this phenotype (Aaskov et al., 2006; Beasley et al., 2004; Shirato et al., 2004).

In lytically infected *Drosophila* cells, a dramatic clustering of mitochondria and FHV RdRp is observed in the perinuclear area

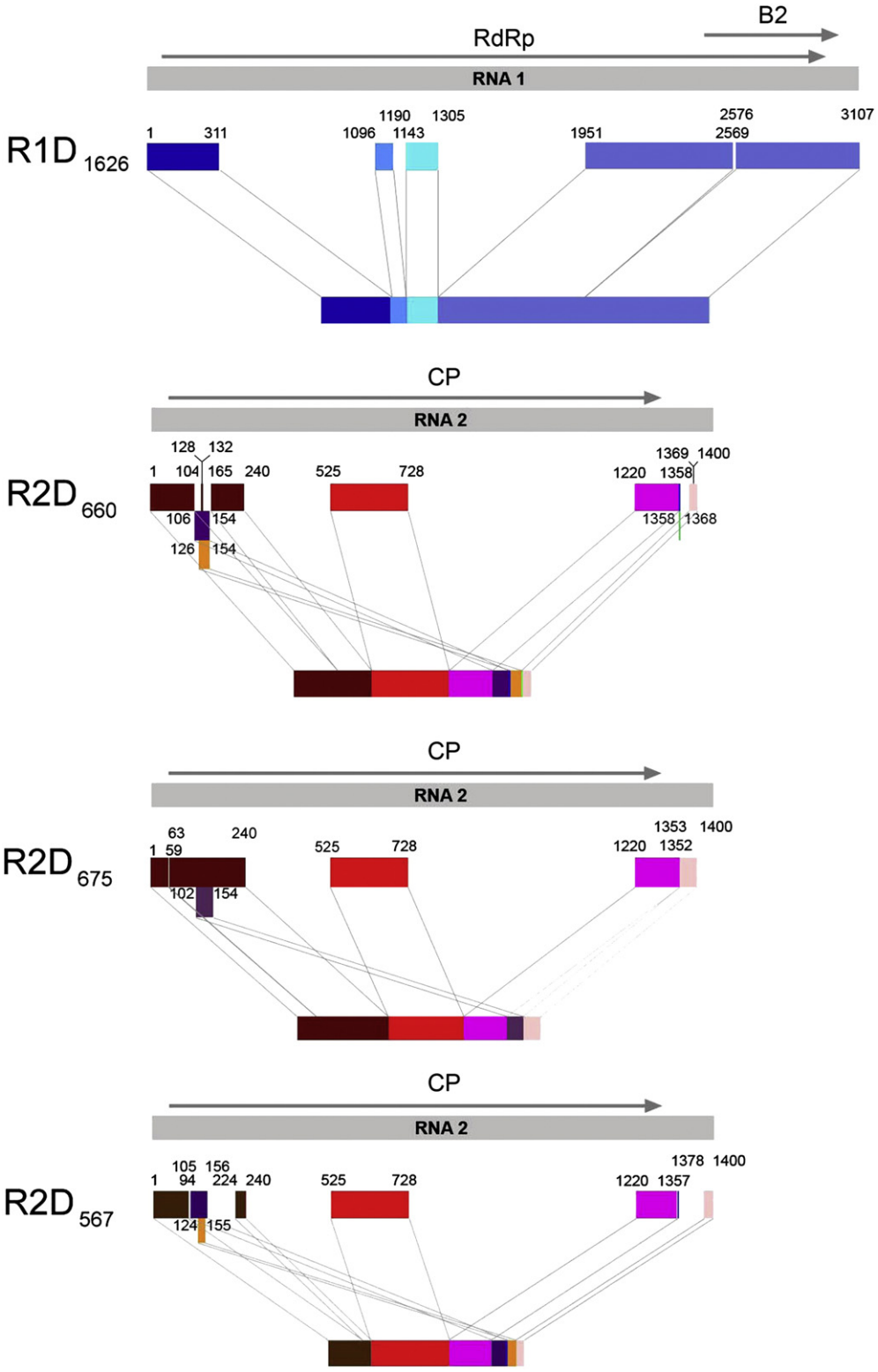

Fig. 5. Primary structure of FHV-derived defective RNA molecules. Schematic diagram of FHV RNA1- and RNA2-derived defective RNA molecules isolated from persistently infected DL-1 cells. The regions of RNA1 and RNA2 retained in the defective RNAs are indicated by numbers representing nucleotide positions in the parent RNAs.

(Miller and Ahlquist, 2002; Venter et al., 2009). In this study, we show for the first time the subcellular distribution of B2 both in LI and PI cells. In LI cells the majority of B2 was detected in close juxtaposition to mitochondria, whereas a smaller fraction was observed in a somewhat reticular pattern in the remainder of the cytoplasm. The predominance of B2 near mitochondria is consistent with its role in binding dsRNA, as viral RNA is synthesized on the outer membrane of these organelles. In fact, it has been reported that B2 co-immunoprecipitates with RdRp (Aliyari et al., 2008), indicating that the two proteins interact. However, it is clear from the immunofluorescence studies reported here, that the fraction of B2 interacting with RdRp must be small and that the majority of the protein, while located in close proximity to mitochondria, is not in direct contact with this organelle and therefore RdRp. It is possible that B2 is bound to

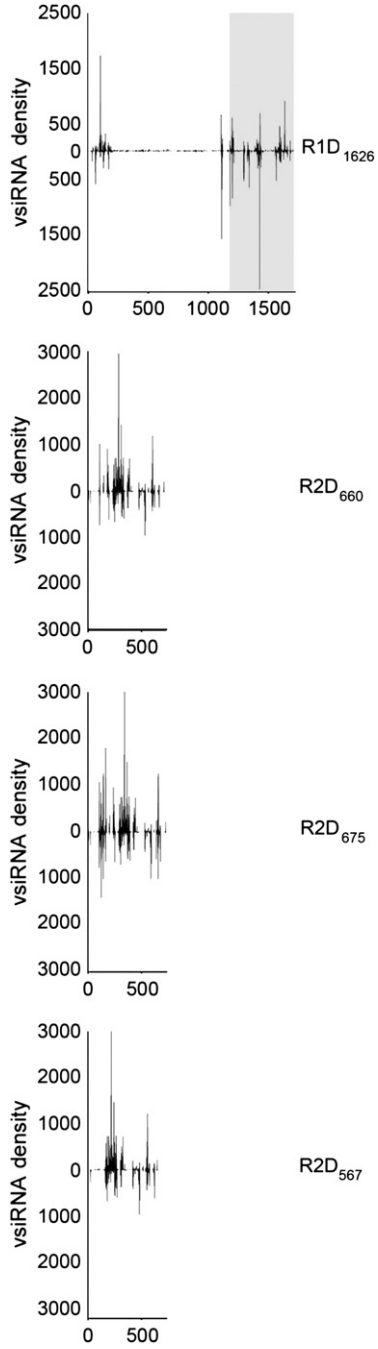

Fig. 6. Density plots of FHV vsiRNAs along the sequence of the defective RNAs. FHV vsiRNAs from persistently infected S2 cells described previously (Czech et al., 2009) were mapped to the sequence of defective RNAs identified in this study. The region that corresponds to RNA3 in wild type RNA1 is shaded gray in $R1D_{1626}$.

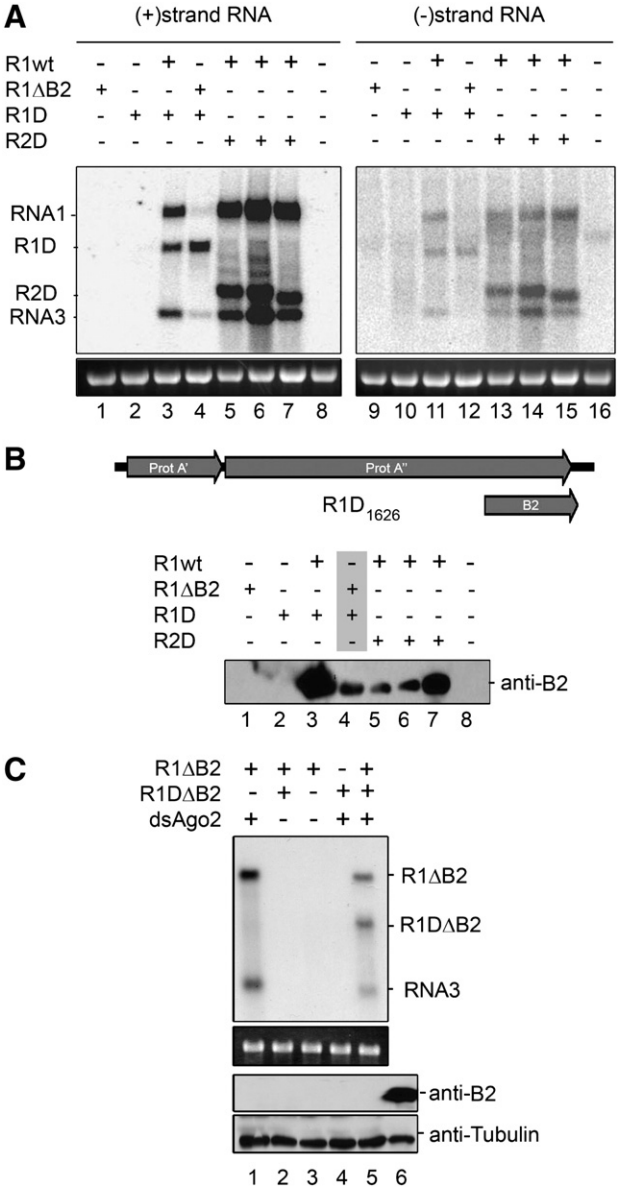

Fig. 7. (A) Evidence for replication of FHV defective RNAs. Naïve DL1 cells were co-transfected with *in vitro* synthesized RNA transcripts indicated above each lane. Total RNA was extracted 48 h later and subjected to Northern blot analysis to detect (+)-sense RNA (lanes 1–8, left panel) and (−)-sense RNA (lanes 9–16, right panel) using the same probes described in the legend of Fig. 1. R1D refers to $R1D_{1626}$. Lanes 5–7 and 13–15 contain $R2D_{660}$, $R2D_{675}$ and $R2D_{567}$ in that order. EtBr-stained rRNA is shown as loading control. (B) Evidence that replication of $R1D_{1626}$ gives rise to protein B2. The top portion shows reading frames present on $R1D_{1626}$ and the putative replication byproduct, subgenomic RNA3. The bottom portion shows an immunoblot blot, in which total cell lysates derived from naïve DL-1 cells transfected as in (A) were probed with a polyclonal antiserum against protein B2 (lanes 1–8). (C) Evidence that replication of $R1D_{1626}$ does not require a B2 open reading frame. DL1 cells were either treated or not treated with dsRNA to silence AGO2 mRNA and inhibit the RNAi pathway. Cells were subsequently transfected with the indicated combinations of *in vitro* transcripts (1 μg each) of R1ΔB2 and R1DΔB2 (lanes 1–5). Top panel: total RNA was extracted 48 h later and analyzed by Northern blot as described in Fig. 1 using a radiolabeled probe spanning nts 2251–3107 of RNA1. Replication of R1DΔB2 is detectable in lane 5 in the absence of B2. Ribosomal RNA is shown as a loading control below the blot. Bottom panel: Western blot of cell lysates derived from the same samples used in the top panel and probed with anti-B2 antiserum to confirm that the transcripts did not revert during replication to give rise to functional B2 protein. Anti-tubulin signal is shown as a loading control. Lane 6 is a positive control for B2 as present in a lysate prepared from $PI_{0.01}$ cells.

progeny viral RNA, protecting it from cleavage as it awaits packaging into particles by capsid protein.

In contrast, in PI cells we did not observe clustering of mitochondria in the perinuclear region and viral proteins appeared distributed in a punctate fashion throughout the cytoplasm. We previously showed that efficient formation of progeny FHV particles requires temporal as well as spatial coordination between viral macromolecules and cellular organelles such as mitochondria and ER (Venter et al., 2005). Although the functional implications of the altered subcellular distribution of the FHV proteins in PI cells awaits further investigation, we speculate that it may represent a suboptimal environment for the events required for production of infectious virus particles.

In summary, our results suggest a complex interaction between the host RNAi response and its suppression during persistent infections. A role for defective RNAs during viral persistence has long been appreciated but is commonly thought to be based on their direct interference with the

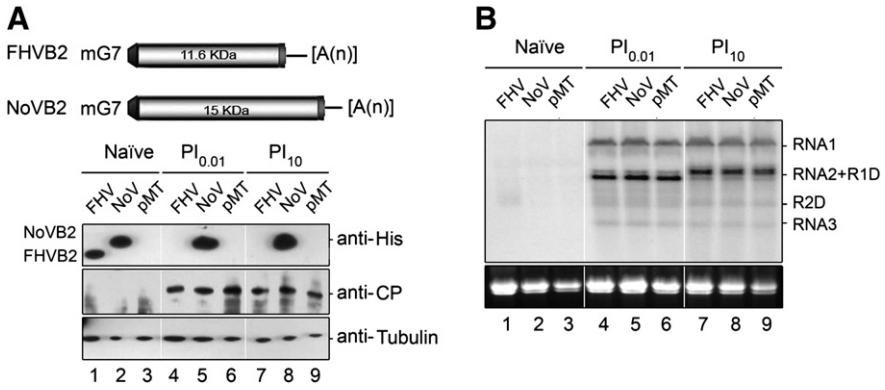

Fig. 8. Effect of exogenous B2 expression on FHV replication in PI cells. (A) The top portion shows a schematic depiction of RNA transcripts derived from plasmid pMT/V5-HisA for exogenous expression of FHV and NoV proteins B2. The His-tag is located at the C terminus of the protein. The bottom portion shows an immunoblot of total cell lysates (lanes 1–9) derived from the indicated cells after transfection with plasmid encoding either the FHV B2 protein, NoV B2 protein or the empty vector. The blots were probed with a monoclonal anti-His antibody for the detection of protein B2, with polyclonal anti-FHV antibodies for the detection of coat protein, and a monoclonal antibody against tubulin as a loading control. Total cell lysates were prepared 72 h post-transfection. (B) Northern blot analysis of total RNA extracted from the indicated cells after transfection with plasmids encoding either the FHV B2 protein, NoV B2 protein or the empty vector (lanes 1–9). Probes used for hybridization were identical to those described in Fig. 1A. EtBr-stained rRNA is shown as a loading control.

replication of genomic length RNAs (Marriot and Dimmock, 2010; Roux et al., 1991; Simon et al., 2004). While this possibility should not be excluded, our data suggest that another role of defective RNAs in viral persistence may be to serve as templates for vsiRNA production thereby maintaining the RNAi loop of this feedback mechanism. Although our results apply to nodaviral persistent infections, they are likely to be operational for other RNA viruses as well.

Experimental procedures

Plasmids

Plasmids used to generate *in vitro* transcripts of FHV RNA1 and RNA2, have been described previously (Schneemann and Marshall, 1998). The MEGAscript kit was used for preparation of *in vitro* transcripts according to the manufacturer's instructions (Ambion). The R1ΔB2 mutant was a kind gift from Dr. Jessica Petrillo, and was created by site-directed mutagenesis of the cDNA of RNA1 using the QuickChange kit (Stratagene). Specifically, a T–C exchange was introduced at nt 2739, which abolished the start codon in the B2 ORF and an additional C–A exchange at position 2910 introduced a premature stop codon in the B2 ORF.

FHV RNA1- and RNA2-derived defective RNAs were amplified using primers that bind to the 5′ and 3′ ends of the parental molecules (for RNA1, p53: gttttcgaaacaaataaaac and p76: acctctgccctttcgggc; for RNA2, p77: gtaaacaattccaagttcc and p88: accttagtctgttgacttaaac). All PCR products of subgenomic length were cloned into the pGEM-T easy vector (Promega) and sequenced.

pDI-eGFP has been described (Dasgupta et al., 2003). For construction of FHVB2-His and NoVB2-His plasmids, each viral sequence was amplified using PCR and primers containing *Eco*RI and *Mlu*I sites, and cloned in-frame with the 6× His epitope of pMT/V5-His A (Invitrogen).

Generation of persistently infected Drosophila cells

DL1 and S2 cells were infected with sucrose gradient-purified FHV at the indicated multiplicities of infection using standard procedures. Cells surviving the infection were continuously cultured in Schneider's insect medium containing 15% heat-inactivated fetal bovine serum and the antibiotics penicillin and streptomycin.

Detection of RNA and proteins by Northern and Western blot analyses, respectively

Detection of RNA molecules was performed as previously described (Jovel et al., 2007), with minor modifications. For mapping of FHV-derived siRNAs, low molecular weight (LMW) RNA from non-infected, LI or PI cells was purified from a 15% PAGE gel containing 8 M Urea. LMW RNA was dephosphorylated with calf intestinal alkaline phosphatase (Invitrogen) and end-labeled with [γ-^{32}P]ATP (3000 Ci/mol; Perkin Elmer). cDNA fragments of ~250 nts [with the exception of fragment 12 (357 nts) and fragment 18 (150 nts)], spanning the entire FHV genome were amplified by PCR using as a template plasmids that contain full-length FHV RNA1 and RNA2 cDNAs (Schneemann and Marshall, 1998). Circa 100 ng of each PCR fragment were run on eight different gels and electroblotted onto nylon membranes, under denaturing conditions (120 mM NaCl, 80 mM NaOH). Membranes were then hybridized against the [γ-^{32}P]ATP-labeled LMW RNAs. Hybridizations of viral RNA and vsiRNA were performed in PerfectHyb Plus buffer (Sigma) at 65 °C and 40 °C, respectively, using the probes described in the legend of each figure. Two post-hybridization washes were conducted at the same temperature in 2× SSC buffer (300 mM NaCl, 30 mM trisodium citrate, pH 7.0) containing 0.5% (w/v) sodium dodecyl sulphate. Radioactive signals were captured using a Storm 820 PhosphorImager (Amersham Biosciences).

Total cellular proteins were fractionated in Nu-PAGE 4–12% Bis–Tris polyacrylamide gels (Invitrogen) and electroblotted onto PVDF (BioRad) membranes. Immunoblotting was performed as described previously (Dong et al., 1998). Mouse monoclonal antibodies were used for detection of 6X-His (Invitrogen) and α-tubulin (Sigma) and rabbit polyclonal antibodies were used for detection of the FHV CP and B2 proteins. The secondary antibodies were either goat anti-mouse or goat anti-rabbit immunoglobulin G conjugated with horseradish peroxidase (GE Healthcare).

RNA silencing and RNA transfection of Drosophila cells

A fragment spanning nucleotides 2211–2855 of AGO2 cDNA (Czech et al. 2008) was amplified with primers flanked by the sequence of the T7 promoter and used to synthesize dsRNA with the MegaScript RNAi kit (Ambion). DL1 cells (5×10^6) were soaked in 1 ml of serum-free *Drosophila* cell culture medium containing 10 μg of dsRNA for 1 h at 27 °C and then supplemented with four volumes of culture medium containing 15% fetal bovine serum. On day four, the soaking procedure was repeated and on day eight cells were transfected with 1 μg each of the indicated combinations of R1ΔB2 and R1DΔB2 *in vitro* transcripts using TransFectin (BioRad). To create the R1DΔB2 mutant, the start codon of the B2 ORF in $R1D_{1626}$ was mutated as described for R1ΔB2.

Immunofluorescence and confocal microscopy

Immunofluorescence detection of FHV proteins and cellular markers was conducted as described (Venter et al., 2009). Briefly, 1.5×10^6 DL-1 PI or LI cells were seeded in concanavalin A-coated 35-mm glass-bottom dishes (MatTek Corp.) and cells were incubated for ~12 h at 27 °C. Cells were then fixed, stained and washed as described (Venter et al., 2009). FHV coat protein was detected with a polyclonal antibody, while the RdRp and B2 proteins were detected with monoclonal antibodies. Fluorescence images were captured using a Zeiss LSM710 inverted confocal laser-scanning microscope.

Acknowledgments

We thank Dr. Jessica Petrillo for generously providing a plasmid encoding R1ΔB2 and Dr. Arno Venter for his continuous support and enthusiastic discussions. We acknowledge Drs. Ranjit Dasgupta and Paul Ahlquist, University of Wisconsin–Madison, for kindly providing plasmid pDIeGFP and RdRp antibodies, respectively. This is manuscript 20,258 from the Scripps Research Institute. The work was supported by NIH grants AI070205 and GM053491 to A.S.

Accession numbers

The sequences of the defective-interfering molecules isolated in this study were deposited in the GenBank under the accession numbers GU393238–GU39324.

References

Aaskov, J., Buzacott, K., Thu, H., Lowry, K., Holmes, E., 2006. Long-term transmission of defective RNA viruses in humans and *Aedes* mosquitoes. Science 311, 236–238.
Aliyari, R., Wu, Q., Li, H.W., Wang, X.H., Li, F., Green, L.D., Han, C.S., Li, W.X., Ding, S.W., 2008. Mechanism of induction and suppression of antiviral immunity directed by virus-derived small RNAs in *Drosophila*. Cell Host Microbe 4, 387–397.
Ball, L.A., Li, Y., 1993. cis-Acting requirements for the replication of flock house virus RNA 2. J. Virol. 67, 3544–3551.
Beasley, D.W., Davis, C.T., Whiteman, M., Granwehr, B., Kinney, R.M., Barrett, A.D., 2004. Molecular determinants of virulence of West Nile virus in North America. Arch. Virol. Suppl. 35–41.
Blair, C.D., 2011. Mosquito RNAi is the major innate immune pathway controlling arbovirus infection and transmission. Future Microbiol. 6, 265–277.
Britt, W., 2008. Manifestations of human cytomegalovirus infection: proposed mechanisms of acute and chronic disease. Curr. Top. Microbiol. Immunol. 325, 417–470.
Carthew, R.W., Sontheimer, E.J., 2009. Origins and mechanisms of miRNAs and siRNAs. Cell 136, 642–655.
Catteau, A., Kalinina, O., Wagner, M.C., Deubel, V., Courageot, M.P., Despres, P., 2003. Dengue virus M protein contains a proapoptotic sequence referred to as ApoptoM. J. Gen. Virol. 84, 2781–2793.
Chao, J.A., Lee, J.H., Chapados, B.R., Debler, E.W., Schneemann, A., Williamson, J.R., 2005. Dual modes of RNA-silencing suppression by Flock House virus protein B2. Nat. Struct. Mol. Biol. 12, 952–957.
Czech, B., Malone, C.D., Zhou, R., Stark, A., Schlingeheyde, C., Dus, M., Perrimon, N., Kellis, M., Wohlschlegel, J.A., Sachidanandam, R., Hannon, G.J., Brennecke, J., 2008. An endogenous small interfering RNA pathway in *Drosophila*. Nature 453, 798–802.
Czech, B., Zhou, R., Erlich, Y., Brennecke, J., Binari, R., Villalta, C., Gordon, A., Perrimon, N., Hannon, G.J., 2009. Hierarchical rules for Argonaute loading in *Drosophila*. Mol. Cell 36, 445–456.
Dasgupta, R., Selling, B., Rueckert, R., 1994. Flock house virus: a simple model for studying persistent infection in cultured *Drosophila* cells. Arch. Virol. Suppl. 9, 121–132.
Dasgupta, R., Cheng, L.L., Bartholomay, L.C., Christensen, B.M., 2003. Flock house virus replicates and expresses green fluorescent protein in mosquitoes. J. Gen. Virol. 84, 1789–1797.
Ding, S.W., 2010. RNA-based antiviral immunity. Nat. Rev. Immunol. 10, 632–644.
Ding, S.W., Voinnet, O., 2007. Antiviral immunity directed by small RNAs. Cell 130, 413–426.
Dong, X.F., Natarajan, P., Tihova, M., Johnson, J.E., Schneemann, A., 1998. Particle polymorphism caused by deletion of a peptide molecular switch in a quasiequivalent icosahedral virus. J. Virol. 72, 6024–6033.
Flynt, A., Liu, N., Martin, R., Lai, E.C., 2009. Dicing of viral replication intermediates during silencing of latent *Drosophila* viruses. Proc. Natl Acad. Sci. USA 106, 5270–5275.
Fuse, S., Molloy, M.J., Usherwood, E.J., 2008. Immune responses against persistent viral infections: possible avenues for immunotherapeutic interventions. Crit. Rev. Immunol. 28, 159–183.
Galiana-Arnoux, D., Dostert, C., Schneemann, A., Hoffmann, J.A., Imler, J.L., 2006. Essential function in vivo for Dicer-2 in host defense against RNA viruses in *Drosophila*. Nat. Immunol. 7, 590–597.
Guarino, L.A., Ghosh, A., Dasmahapatra, B., Dasgupta, R., Kaesberg, P., 1984. Sequence of the black beetle virus subgenomic RNA and its location in the viral genome. Virology 139, 199–203.
Hammond, S.M., Boettcher, S., Caudy, A.A., Kobayashi, R., Hannon, G.J., 2001. Argonaute2, a link between genetic and biochemical analyses of RNAi. Science 293, 1146–1150.
Horwich, M.D., Li, C., Matranga, C., Vagin, V., Farley, G., Wang, P., Zamore, P.D., 2007. The *Drosophila* RNA methyltransferase, DmHen1, modifies germline piRNAs and single-stranded siRNAs in RISC. Curr. Biol. 17, 1265–1272.
Huszar, T., Imler, J.L., 2008. *Drosophila* viruses and the study of antiviral host-defense. Adv. Virus Res. 72, 227–265.
Jovel, J., Walker, M., Sanfacon, H., 2007. Recovery of *Nicotiana benthamiana* plants from a necrotic response induced by a nepovirus is associated with RNA silencing but not with reduced virus titer. J. Virol. 81, 12285–12297.
Kemp, C., Imler, J.L., 2009. Antiviral immunity in *Drosophila*. Curr. Opin. Immunol. 21, 3–9.
Kim, K., Lee, Y.S., Harris, D., Nakahara, K., Carthew, R.W., 2006. The RNAi pathway initiated by Dicer-2 in *Drosophila*. Cold Spring Harb. Symp. Quant. Biol. 71, 39–44.
Kim, K., Lee, Y.S., Carthew, R.W., 2007. Conversion of pre-RISC to holo-RISC by Ago2 during assembly of RNAi complexes. RNA 13, 22–29.
Korber, S., Shaik Syed Ali, P., Chen, J.C., 2009. Structure of the RNA-binding domain of Nodamura virus protein B2, a suppressor of RNA interference. Biochemistry 48 (11), 2307–2309.
Kuno, G., 2001. Persistence of arboviruses and antiviral antibodies in vertebrate hosts: its occurrence and impacts. Rev. Med. Virol. 11, 165–190.
Lanman, J., Crum, J., Deerinck, T.J., Gaietta, G.M., Schneemann, A., Sosinsky, G.E., Ellisman, M.H., Johnson, J.E., 2008. Visualizing flock house virus infection in *Drosophila* cells with correlated fluorescence and electron microscopy. J. Struct. Biol. 161, 439–446.
Lee, Y.S., Nakahara, K., Pham, J.W., Kim, K., He, Z., Sontheimer, E.J., Carthew, R.W., 2004. Distinct roles for *Drosophila* Dicer-1 and Dicer-2 in the siRNA/miRNA silencing pathways. Cell 117, 69–81.
Li, Y., Ball, L.A., 1993. Nonhomologous RNA recombination during negative-strand synthesis of flock house virus RNA. J. Virol. 67, 3854–3860.
Liu, Q., Rand, T.A., Kalidas, S., Du, F., Kim, H.E., Smith, D.P., Wang, X., 2003. R2D2, a bridge between the initiation and effector steps of the *Drosophila* RNAi pathway. Science 301, 1921–1925.
Marques, J.T., Kim, K., Wu, P.H., Alleyne, T.M., Jafari, N., Carthew, R.W., 2010. Loqs and R2D2 act sequentially in the siRNA pathway in *Drosophila*. Nat. Struct. Mol. Biol. 17, 24–30.
Marriot, A.C., Dimmock, N.J., 2010. Defective interfering viruses and their potential as antiviral agents. Rev. Med. Virol. 20, 51–62.
Miller, D.J., Ahlquist, P., 2002. Flock house virus RNA polymerase is a transmembrane protein with amino-terminal sequences sufficient for mitochondrial localization and membrane insertion. J. Virol. 76, 9856–9867.
Miller, D.J., Schwartz, M.D., Ahlquist, P., 2001. Flock house virus RNA replicates on outer mitochondrial membranes in *Drosophila* cells. J. Virol. 75, 11664–11676.
Okamura, K., Robine, N., Liu, Y., Liu, Q., Lai, E.C., 2011. R2D2 organizes small regulatory RNA pathways in *Drosophila*. Mol. Cell. Biol. 31, 884–896.
Oldstone, M.B., 2006. Viral persistence: parameters, mechanisms and future predictions. Virology 344, 111–118.
Prikhod'ko, G.G., Prikhod'ko, E.A., Cohen, J.I., Pletnev, A.G., 2001. Infection with Langat flavivirus or expression of the envelope protein induces apoptotic cell death. Virology 286, 328–335.
Rand, T.A., Petersen, S., Du, F., Wang, X., 2005. Argonaute2 cleaves the anti-guide strand of siRNA during RISC activation. Cell 123, 621–629.
Roux, L., Simon, A., Holland, J.J., 1991. Effects of defective interfering viruses on virus replication and pathogenesis. Adv. Virus Res. 40, 181–211.
Schneemann, A., Marshall, D., 1998. Specific encapsidation of nodavirus RNAs is mediated through the C terminus of capsid precursor protein alpha. J. Virol. 72, 8738–8746.
Scotti, P.D., Dearing, S., Mossop, D.W., 1983. Flock house virus: a nodavirus isolated from *Costelytra zealandica* (White) (Coleoptera: Scarabaeidae). Arch. Virol. 75, 181–189.
Selling, B.H., 1986. Infectivity of Black Beetle Virus in Cultured *Drosophila* Cells. PhD thesis University of Wisconsin, Madison.
Shirato, K., Miyoshi, H., Goto, A., Ako, Y., Ueki, T., Kariwa, H., Takashima, I., 2004. Viral envelope protein glycosylation is a molecular determinant of the neuroinvasiveness of the New York strain of West Nile virus. J. Gen. Virol. 85, 3637–3645.
Simon, A.E., Roossinck, M.J., Havelda, Z., 2004. Plant virus satellite and defective interfering RNAs: new paradigms for a new century. Annu. Rev. Phytopathol. 42, 415–437.
van Rij, R.P., Berezikov, E., 2009. Small RNAs and the control of transposons and viruses in *Drosophila*. Trends Microbiol. 17, 163–171.
van Rij, R.P., Saleh, M.C., Berry, B., Foo, C., Houk, A., Antoniewski, C., Andino, R., 2006. The RNA silencing endonuclease Argonaute 2 mediates specific antiviral immunity in *Drosophila* melanogaster. Genes Dev. 20, 2985–2995.
Venter, P.A., Krishna, N.K., Schneemann, A., 2005. Capsid protein synthesis from replicating RNA directs specific packaging of the genome of a multipartite, positive-strand RNA virus. J. Virol. 79, 6239–6248.
Venter, P.A., Marshall, D., Schneemann, A., 2009. Dual roles for an arginine-rich motif in specific genome recognition and localization of viral coat protein to RNA replication sites in flock house virus-infected cells. J. Virol. 83, 2872–2882.
Wang, X.H., Aliyari, R., Li, W.X., Li, H.W., Kim, K., Carthew, R., Atkinson, P., Ding, S.W., 2006. RNA interference directs innate immunity against viruses in adult *Drosophila*. Science 312, 452–454.
Wu, Q., Luo, Y., Lu, R., Lau, N., Lai, E.C., Li, W.X., Ding, S.W., 2010. Virus discovery by deep sequencing and assembly of virus-derived small silencing RNAs. Proc. Natl Acad. Sci. USA 107, 1606–1611.
Zhong, W., Dasgupta, R., Rueckert, R., 1992. Evidence that the packaging signal for nodaviral RNA2 is a bulged stem-loop. Proc. Natl Acad. Sci. USA 89, 11146–11150.